- Supplementary Material -

Ethanol condensation at elevated pressure over copper on AlMgO and AlCaO porous mixed-oxide supports

Davi D. Petrolini[1,+], Nathaniel Eagan[2,+], Madelyn R. Ball[2], Samuel P. Burt[2], Ive Hermans[2], George W. Huber[2], James A. Dumesic[2] and Leandro Martins[1,*]

[1] *Instituto de Química, Unesp - Universidade Estadual Paulista, R. Prof. Francisco Degni 55, 14800-900 Araraquara, SP, Brazil*

[2] *Department of Chemical and Biological Engineering, University of Wisconsin-Madison, 1415 Engineering Drive, Madison, Wisconsin 53706, United States*

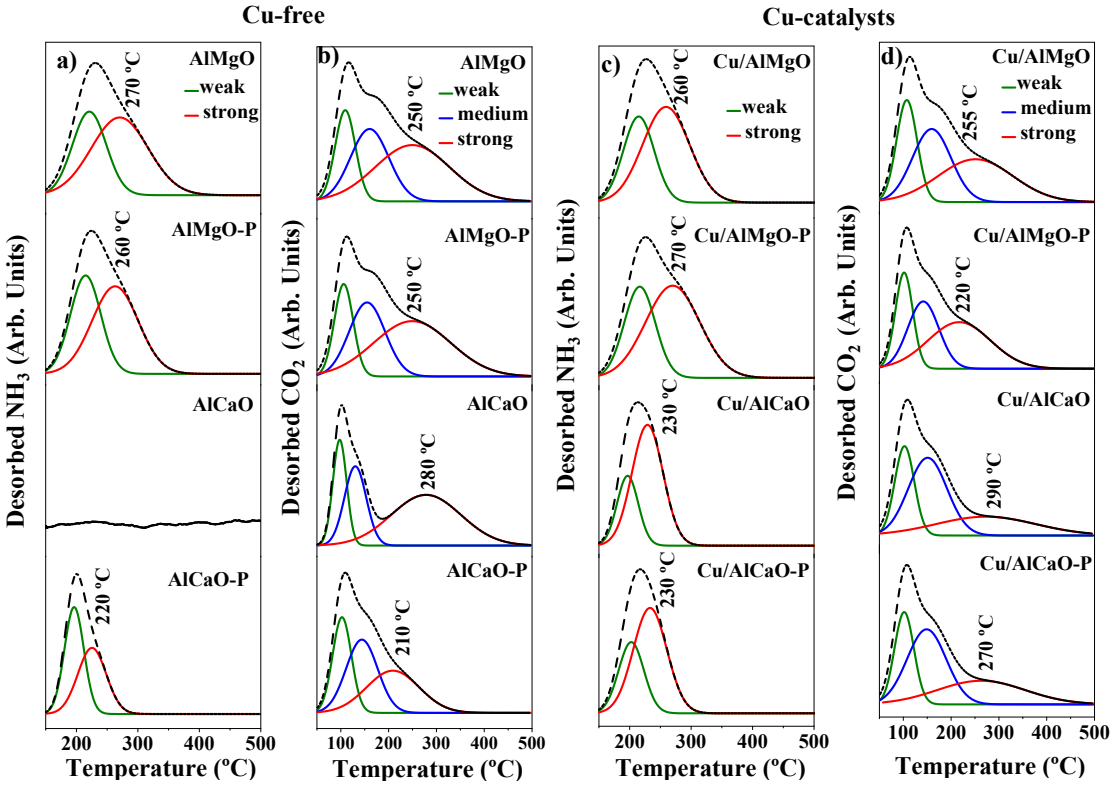

Fig. S1. Deconvolutions of (a, c) NH_3-TPD profiles and (b, d) CO_2-TPD profiles of Cu-free and Cu-catalysts.

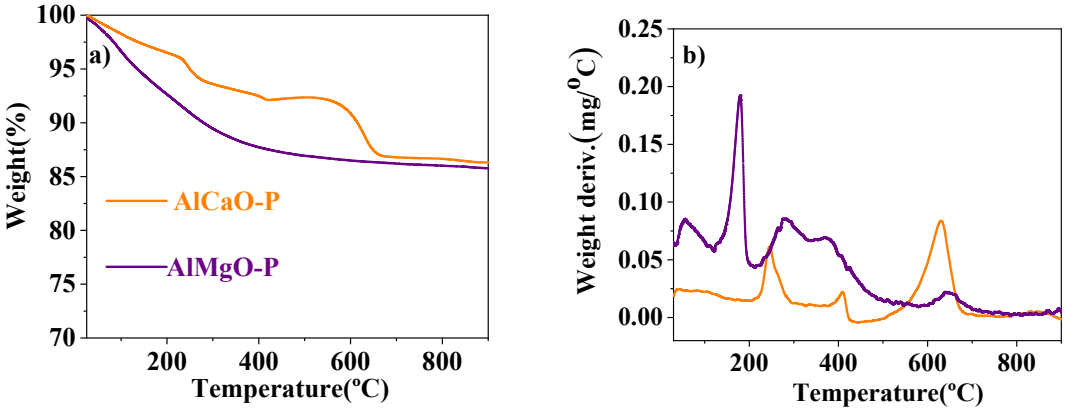

Fig. S2. a) Thermogravimetric curves; b) weight derivative for calcined and exposed to atmospheric environment AlMgO-P and AlCaO-P catalysts.

Table S1. BET area, Cu loading, Cu particle size, Cu^0 site density, and distribution of strengths of surface acid and basic sites.

Sample	BET area (m^2/g)	Cu loading[a] (%)	Cu particle size[b] (nm)	Cu^0 sites[c] (μmol/g)	Acid site distribution[d]			Base site distribution[e]			
					Weak (%)	Strong (%)	Total NH_3 (μmol/g)	Weak (%)	Medium (%)	Strong (%)	Total CO_2 (μmol/g)
Cu/AlMgO	106	8.0	3.7	67	37.1	62.9	92.9	25.9	34.6	39.5	115
Cu/AlMgO-P	171	8.0	2.1	91	36.2	63.8	106	25.1	31.2	43.7	78.6
Cu/AlCaO	102	9.0	2.6	118	28.3	71.7	10.1	26.3	45.4	28.4	52.4
Cu/AlCaO-P	120	9.6	3.1	140	33.6	66.4	12.5	26.3	43.1	30.6	49.7
AlMgO	191	-		-	52.6	47.4	76.9	20.9	31.5	47.6	192
AlMgO-P	315	-		-	42.6	57.4	85.6	20.1	30.7	49.2	238
AlCaO	133	-		-	-	-	-*	16.4	36.9	46.7	43.8
AlCaO-P	202	-		-	52.6	47.4	4.0	28.4	36.5	35.1	46.9

[a] Cu loading determined by ICP.
[b] Cu particle sizes obtained from STEM.
[c] Metallic copper sites quantified by N_2O chemisorption.
[d]Acid sites quantified from NH_3-TPD profiles.
[e]Base sites quantified with CO_2-TPD profiles.
*Without significant acidity.

Table S2. Ethanol (EtOH) dehydrogenation to acetaldehyde (AcAl) equilibrium as a function of pressure compared to experiment. y_{AcAl} is the molar concentration of AcAl in the gas. Temperature = 325°C, EtOH feed concentration = 12.3 vol%, balance H_2.

Pressure (bar)	**1-H_2**	**10-H_2**	**24-H_2**	**31-H_2**	**31-Ar**
Equilibrium					
AcAl yield (C%)	55.0	11.1	4.9	3.9	42.0
P_{AcAl} (kPa)	6.40	13.43	14.49	14.67	151.7
y_{AcAl} (mol%)	6.3	1.3	0.6	0.5	4.9
AcAl:EtOH (mol/mol)	1.22	0.13	0.05	0.04	0.72
Experiment					
AcAl yield (C%)	10.1	5.6	2.9	2.5	4.4
P_{AcAl} (kPa)	1.2	6.9	8.4	9.7	17.0
y_{AcAl} (mol%)	1.2	0.7	0.4	0.3	0.5
AcAl:EtOH (mol/mol)	0.12	0.07	0.04	0.03	0.07

Table S3. Data collected from literature for catalysts, reactions conditions, conversion and selectivity for Guerbert coupling. *Nominal WHSV were calculated for batch reactions for approximate comparison with flow studies.

Catalyst	T (ºC)	P (bar)	WHSV* (h^{-1})	Flow or Batch	Gas Cofeed	Conv. (%)	Sel. (%) to n-butanol	Ref.
AlMgO	325	32	2.1	flow	H_2	7.1	28.4	This work
AlMgO-P	325	32	2.1	flow	H_2	11.1	36.2	
Cu/AlMgO	325	32	2.1	flow	H_2	19.7	48.7	
Cu/AlMgO-P	325	32	2.1	flow	H_2	23.3	43.3	
Cu/AlMgO-P	325	32	0.7	flow	H_2	32.8	35.8	
AlCaO	325	32	2.1	flow	H_2	0.2	42.7	
AlCaO-P	325	32	2.1	flow	H_2	0.2	61.6	
Cu/AlCaO	325	32	2.1	flow	H_2	8.7	20.4	
Cu/AlCaO-P	325	32	2.1	flow	H_2	8.4	21.4	
MgAlOx	250	30	3.2	flow	N_2	0.2	57.1	[1]
NiMgAlOx	300	30	3.2	flow	N_2	27.9	45.1	[1]
MgAlOx	200	30	3.5	batch	N_2	3.6	50.5	[2]
Pd/MgAlOx/0.25Ga	200	30	3.5	batch	N_2+H_2	11.6	94.0	[2]
Pt/MgAlOx	200	30	3.5	batch	N_2	13.0	82.0	[2]
Cu/AlMgO	310	80	23.7	batch	Ar	37.8	22.0	[3]
Ni/AlMgO	310	80	23.7	batch	Ar	30.3	73.0	[3]
Cu/Ni-AlMgO	310	80	23.7	batch	Ar	47.9	72.0	[3]
MgO	360	2	-	flow	N_2	4.4	33.0	[4]
$Ca_{10}(PO_4)_6(OH)_2$	360	2	-	flow	N_2	4.9	72.0	[4]
$Sr_3(PO_4)_2$	360	2	-	flow	N_2	4.2	9.0	[4]
CuMgAl	300	1	23.7	batch	N_2	46.5	62.2	[5]
Pd-CuMgAl	260	1	23.7	batch	N_2	20.9	45.5	[5]
In-CuMgAl	260	1	23.7	batch	N_2	26.6	60.0	[5]
Ni/γ-alumina	250	180	6.4	flow	He	35.0	61.7	[6]
Ni/Al_2O_3	250	100	23.9	batch	He	25.0	80.0	[7]
Au/Al_2O_3	250	100	23.9	batch	He	6	35	[7]
$Cu_{10}MgAl_3O$	200	autogenic	78.9	batch	-	4.5	28.0	[8]
Ag_5MgAlO	200	autogenic	78.9	batch	-	1.6	38.8	[8]
Mn_5MgAlO	200	autogenic	78.9	batch	-	0.7	53.3	[8]
Fe_5MgAlO	200	autogenic	78.9	batch	-	0.3	39.2	[8]
Sm_5MgAlO	200	autogenic	78.9	batch	-	1.3	66.3	[8]
Yb_5MgAlO	200	autogenic	78.9	batch	-	1.2	53.0	[8]
Mg_1Al_1O	350	1	-	flow	N_2	40.5	22.0	[9,10]
Mg_3Al_1O	350	1	-	flow	N_2	33.2	34.2	[9,10]
$Cu_5MgAl_{(1)}O$	200	autogenic	78.9	batch	-	7.3	50.5	[11]

[1] J. Pang, M. Zheng, L. He, L. Li, X. Pan, A. Wang, X. Wang, T. Zhang, Upgrading ethanol to n-butanol over highly dispersed Ni-MgAlO catalysts, J. Catal. 344 (2016) 184-193.

[2] ANTOLÍN, Ricardo Arjona et al. Method for obtaining higher alcohols. U.S. Patent n. 9,475,741, 25 out. 2016.

[3] SUN, Zhuohua et al. Efficient Catalytic Conversion of Ethanol to 1-Butanol via the Guerbet Reaction over Copper-and Nickel-Doped Porous. ACS Sustainable Chemistry & Engineering, v. 5, n. 2, p. 1738-1746, 2016.

[4] HANSPAL, Sabra et al. Influence of surface acid and base sites on the Guerbet coupling of ethanol to butanol over metal phosphate catalysts. Journal of Catalysis, v. 352, p. 182-190, 2017.

[5] PERRONE, Olavo Micali et al. Butanol synthesis from ethanol over CuMgAl mixed oxides modified with palladium (II) and indium (III). Fuel Processing Technology, v. 177, p. 353-357, 2018.
[6] GHAZIASKAR, Hassan S.; XU, Chunbao Charles. One-step continuous process for the production of 1-butanol and 1-hexanol by catalytic conversion of bio-ethanol at its sub-/supercritical state. RSC Advances, v. 3, n. 13, p. 4271-4280, 2013.
[7] RIITTONEN, Toni et al. One-pot liquid-phase catalytic conversion of ethanol to 1-butanol over aluminium oxide-the effect of the active metal on the selectivity. Catalysts, v. 2, n. 1, p. 68-84, 2012.
[8] MARCU, Ioan-Cezar et al. Catalytic conversion of ethanol into butanol over M–Mg–Al mixed oxide catalysts (M= Pd, Ag, Mn, Fe, Cu, Sm, Yb) obtained from LDH precursors. Catalysis letters, v. 143, n. 1, p. 23-30, 2013.
[9] DI COSIMO, Juana Isabel et al. Structural requirements and reaction pathways in condensation reactions of alcohols on MgyAlOx catalysts. Journal of Catalysis, v. 190, n. 2, p. 261-275, 2000.
[10] WU, Xianyuan et al. Catalytic Upgrading of Ethanol to n-Butanol: Progress in Catalyst Development. ChemSusChem, v. 11, n. 1, p. 71-85, 2018.
[11] MARCU, Ioan-Cezar et al. Catalytic valorization of bioethanol over Cu-Mg-Al mixed oxide catalysts. Catalysis Today, v. 147, n. 3-4, p. 231-238, 2009.

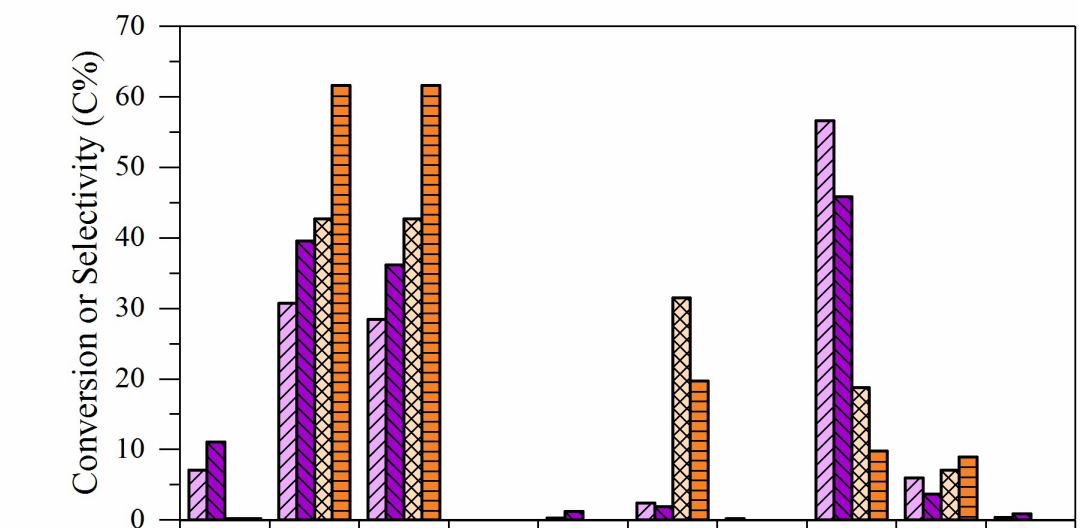

	Conv.	Desired	nButOH	ButAl	C_{6+} Ald/Alc	AcAl	EtOAc	DEE	EtEn/An	C_{4+} AlkEn/An
AlMgO	7.1	30.7	28.4	0.0	0.3	2.4	0.2	56.6	5.9	0.3
AlMgO-P	11.1	39.5	36.2	0.0	1.2	1.9	0.0	45.8	3.6	0.9
AlCaO	0.2	42.7	42.7	0.0	0.0	31.5	0.0	18.7	7.0	0.0
AlCaO-P	0.2	61.6	61.6	0.0	0.0	19.7	0.0	9.8	9.0	0.0

Fig. S3. Conversion and selectivities to major species in ethanol conversion over Cu-free catalysts. Conditions: 325°C, 225 mg catalyst, 10 μL min^{-1} ethanol, 30 mL min^{-1} H_2, 32 bar total pressure.

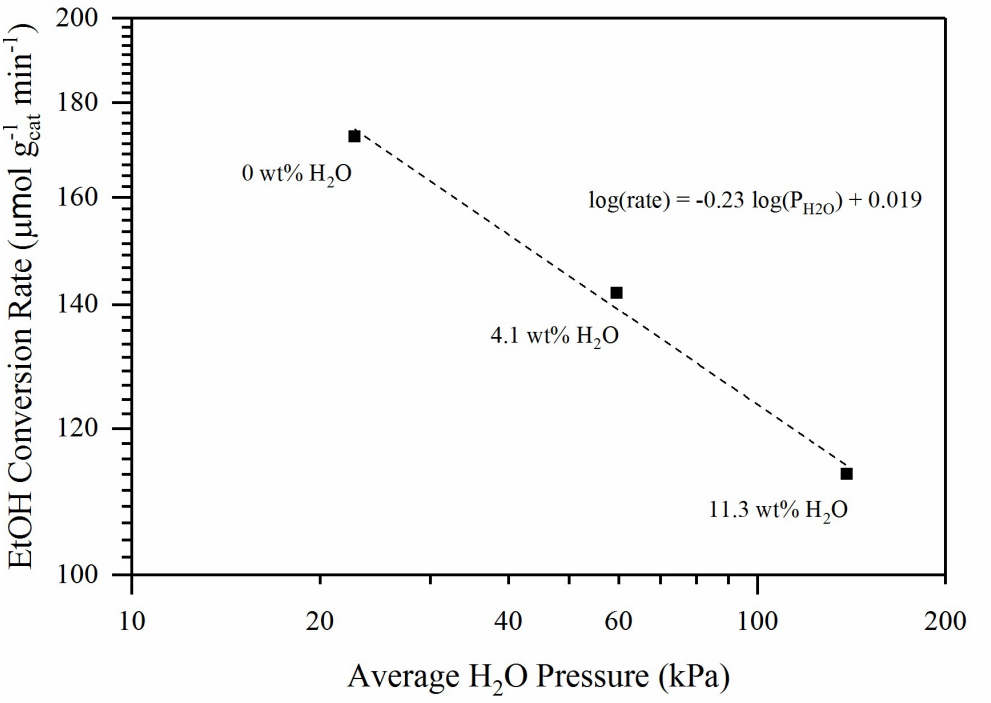

Fig. S4. Ethanol conversion rate vs. the average partial pressure of water across the catalyst bed calculated based upon the observed products and assumed reaction stoichiometries. The log-log plot provides a rate order for water of -0.23 with respect to ethanol conversion.

Transport Calculations:

The possibility that reaction rates were limited by heat or mass transport was examined through evaluation of several transport criteria which must be satisfied to ensure that this is not the case. These criteria have been notably applied and discussed by Shabaker et al. The criteria considered and their evaluations are shown below. Descriptions and approximations for each parameter are also provided. Ethanol condensation to 1-butanol and water was assumed to be the main reaction when one was required for estimation purposes, such as for the absolute heat of reaction. For parameters which were not measured, worst-case approximations were assumed (e.g. a high activation barrier, low particle thermal conductivity, high rate order). **In all cases, the tests were satisfied by multiple orders of magnitude.**

J.W. Shabaker, R.R. Davda, G.W. Huber, R.D. Cortright, J.A. Dumesic, Aqueous-phase reforming of methanol and ethylene glycol over alumina-supported platinum catalysts, J. Catal. 215 (2003) 344-352.

Test	**Equation**	**Evaluation**
Interphase heat transport	$\frac{q\,R\,r_p}{h\,T_B} < 0.15\frac{R\,T_B}{E}$	$3.98 * 10^{-5} \ll 7.46 * 10^{-8}$
Intraparticle heat transport	$\frac{q\,R\,r_p^2}{\lambda\,T_S} < 0.75\frac{R\,T_S}{E}$	$3.83 * 10^{-5} \ll 3.73 * 10^{-7}$
Interphase mass transport	$\frac{R\,r_p^2}{C_b k_c} < \frac{0.15}{n}$	$3.28 * 10^{-8} \ll 7.50 * 10^{-2}$
Intraparticle mass transport	$\frac{R\,r_p^2}{C_s D_{eff}} < 0.3$	$3.33 * 10^{-4} \ll 3.00 * 10^{-1}$

Parameter	**Definition**	**Approximate Value**
q	Absolute heat of reaction	$21{,}517\ J\ mol^{-1}\ ethanol$
R	Volumetric reaction rate	$8.86\ mol\ m^{-3}\ s^{-1}$
r_p	Catalyst particle radius	$1.25 * 10^{-4}\ m$
R	Gas constant	$8.314\ J\ mol^{-1} K^{-1}$
T_B	Bulk temperature	$598\ K$
T_S	Catalyst surface temperature	$598\ K$
h	Heat transfer coefficient	$1000\ W\ m^{-2} K^{-1}$
E	Activation barrier	$100{,}000\ J\ mol^{-1} K^{-1}$
λ	Thermal conductivity of catalyst particle	$0.13\ W\ m^{-1}\ K^{-1}$
C_b	Bulk concentration of ethanol	$79.1\ mol\ ethanol\ m^{-3}$
C_s	Ethanol surface concentration	$79.1\ mol\ ethanol\ m^{-3}$
k_c	Surface-bulk mass transfer coefficient	$5.34 * 10^{-2}\ m\ s^{-1}$
n	Rate order	2
D_{eff}	Effective diffusivity	$5.25 * 10^{-6}\ m^2\ s^{-1}$